Food Hydrocolloids 138 (2023) 108466

Contents lists available at ScienceDirect

Food Hydrocolloids

journal homepage: www.elsevier.com/locate/foodhyd

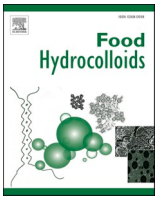

Structural and functional differences between ice crystal-dominated and fat network-dominated ice cream

Xiangyu Liu, Guido Sala, Elke Scholten *

Physics and Physical Chemistry of Foods, Wageningen University, Bornse Weilanden 9, 6708 WG, Wageningen, the Netherlands

ARTICLE INFO

Keywords:
Ice cream microstructure
X-ray tomography
Liquid nitrogen
Overrun
Ice crystal size

ABSTRACT

In this study, we investigated the effect of overrun, fat destabilization degree and ice crystal size on viscoelastic behavior, hardness and melting properties of ice cream by changing only one parameter at a time. To vary the degree of fat destabilization, we changed the emulsifier type; to modify overrun and ice crystal size, we used either a batch freezer or liquid nitrogen freezing upon whipping. Fat destabilization degree, overrun and ice crystal size were measured to determine the structural differences between the studied samples. Furthermore, viscoelastic behavior upon increasing strain and temperature were evaluated by oscillatory rheology. Hardness and meltdown tests were performed to explore the role of different microstructural elements. Depending on the composition of the ice cream, we identified two main types of structures: one dominated by the ice crystals, and one dominated by a fat network. The results showed that the ice crystal-dominated structure contributed more than the fat network to viscoelastic behavior and hardness, whereas the fat network had a larger effect on the melting process. Only a limited effect of ice crystal size on the properties of the ice cream was seen, independently of the kind of dominated structure. In both types of ice cream, overrun had a large effect on mechanical properties, but only in ice crystal-dominated samples it also affected melting. This research provides a better understanding of the role of multiple structural elements in ice cream, which can be used for its reformulation.

1. Introduction

Ice cream is generally described as having "a complex microstructure consisting of air cells, ice crystals, and a network of coalesced fat droplets entrapped in a thick continuous phase" (Scholten, 2014). The structural elements in ice cream can be divided into four categories: (1) fat phase (fat content and degree of fat destabilization), (2) air phase (air cell size and overrun), (3) ice phase (ice crystal size and ice fraction), and (4) unfrozen serum phase. Among these structural elements, fat content and ice fraction can be easily controlled by adding different amounts of fat and varying the ratio between sugar and water, which also determines the final unfrozen serum phase. In addition, the concentration and the type of emulsifier influence the degree of fat destabilization. The addition of emulsifiers helps to destabilize the emulsion, as they are claimed to displace proteins from the interface, thereby creating a thinner interface favoring coalescence. This increases the extent of fat partial coalescence and also influences overrun (Warren & Hartel, 2018). However, many factors in ice cream do not just depend on the composition, but also on the production process. For example, the shear stresses exerted during the freezing process influence the size of the air cells (Chang & Hartel, 2002), that of the ice crystals (Russell, Cheney, & Wantling, 1999), and fat destabilization (Goff & Jordan, 1989). In addition, the rate of cooling leads to faster ice crystallization, which also has an effect on the final ice crystal size. The microstructure of ice cream depends therefore on both its composition and production process.

The microstructure of ice cream is responsible for its viscoelastic behavior, hardness and melting properties, which are important quality parameters. For example, the fat network formed by fat aggregates has been shown to greatly decrease the melting rate of ice cream and promote shape retention (Tharp, Forrest, Swan, Dunning, & Hilmoe, 1998; Warren & Hartel, 2014). Also the overrun and the ice crystal size can influence melting. The melting behavior is governed by the heat transfer from the warmer environment to the ice cream. As air is a good insulator, ice cream with low overrun has been found to melt quickly, whereas ice creams with high overrun have a good melting resistance (Warren et al., 2018). However, this contradicts the results found by Muse and Hartel (2004), who showed that overrun did not appear to

* Corresponding author.
E-mail address: elke.scholten@wur.nl (E. Scholten).

https://doi.org/10.1016/j.foodhyd.2023.108466
Received 27 October 2022; Received in revised form 20 December 2022; Accepted 4 January 2023
Available online 5 January 2023

affect the melting rate. Heat transfer is also in part affected by the ice crystals, but also in this case conflicting results can be found in literature. Muse et al. (2004) found that the melting rate increased as ice crystal size increased, which was attributed to the less tortuous flow path of the serum phase created by large ice crystals. However, no clear correlation could be found between ice crystal size and melting rate in the study of Amador, Hartel, and Rankin (2017). Even though many studies have been performed, the contradictory indications reported in literature show that there is still limited understanding of how the microstructural factors of ice cream influence melting. This is often related to the fact that in published studies many parameters are changed at the same time, which makes it challenging to extract their exact effects.

Besides melting, also hardness is an important quality parameter of ice cream. The hardness of ice cream is affected by overrun, ice crystal size and fat network. Also for hardness, contradictory results related to air content have been reported (Muse et al., 2004; Prindiville, Marshall, & Heymann, 1999). This was attributed to differences in secondary effects (ice crystal size, etc.), highlighting again that information on the role of the individual microstructural features of ice cream is difficult to obtain. Also in the case of ice crystal size, conflicting results were found (Sakurai, 1996; Sofjan & Hartel, 2004). In some cases, larger ice crystals have been shown to increase hardness, while in others they lead to a decrease in hardness. Contradicting results have also been seen for the effect of the degree of fat destabilization. Destabilized fat was found to provide a network among the air cells in ice cream, thereby increasing hardness (Muse et al., 2004). However, another research showed that no significant correlation was found between destabilized fat and hardness. This was again attributed to a secondary effect, as differences in ice crystal size were also found (Amador et al., 2017). Overall, it is clear that each structural element (overrun, fat destabilization degree and ice crystal size), individually or in concomitance with others, affects viscoelastic behavior, hardness and melting properties of ice cream. However, it is difficult to gain insight into the relative importance of the different structural elements on these properties. For a better understanding of the physics of ice cream, these elements have to be controlled separately.

The main aim of this study was to unveil the individual role of fat network, overrun and ice crystal size in determining viscoelastic behavior, hardness and melting properties of ice cream by changing only one of these characteristics at a time, while keeping the others constant. To manipulate the degree of fat destabilization and thus alter the fat network, two different surfactants were chosen. Tween 80 served as the emulsifier to induce fat aggregation or partial coalescence. On the other hand, whey protein isolate (WPI) was used to strongly stabilize the fat droplets, resulting in limited fat destabilization. Furthermore, two freezing methods, a batch freezer or freezing with liquid nitrogen, were used to manipulate overrun and ice crystal size. Fat content and viscosity of the unfrozen serum phase were kept constant. In addition, sugar type and ratio sugar: water were kept the same in all ice creams to guarantee that all samples had the same ice fraction. Fat destabilization degree, overrun and ice crystal size were measured separately to characterize the microstructural differences between the studied samples. X-Ray Tomography (XRT) was used to visualize the structural differences of ice creams with different overrun levels. Furthermore, we applied strain sweep and temperature sweep oscillatory rheology to identify the structure changes during small deformation and melting. Hardness tests were performed to explore the role of different microstructural elements at large deformation. The meltdown properties of samples were also determined to clarify the effect of different structural elements on melting.

2. Materials and methods

2.1. Materials

Anhydrous milk fat was kindly donated by FrieslandCampina (Wageningen, Netherlands). Whey protein isolate (WPI, 88.8% protein content) was purchased from Davisco (USA). Tween 80 (P4780) and sucrose were both purchased from Signa-Aldrich (Netherlands). Kerosene was purchased from a local store (Action, Wageningen, Netherlands). Liquid nitrogen was obtained from SOL GROUP (the Netherlands). Ultrapure water, purified by a Millipore Milli-Q system (Darmstadt, Germany), was used for the preparation of all samples.

2.2. Mix preparation

Two emulsions containing either Tween 80 or WPI as emulsifier were prepared. For the Tween 80-stabilized emulsion, a stock emulsion of 12% AMF was prepared. AMF was melted at 65 °C and then added to a 0.3% (w/w) Tween 80 solution containing 16.55% sucrose. For the WPI emulsion, WPI (4%) was added to water while stirring and was allowed to hydrate for 1 h at room temperature. AMF was melted at 65 °C, and was added at a concentration of 12% to the WPI solution containing 15.85% sucrose. Both emulsions were prepared by pre-homogenization with an Ultra Turrax at a speed of 13,000 rpm for 2 min and then homogenized by a homogenizer (Delta Instruments LaboScope Homogenizer HU-3.0, USA) at 13 MPa for one cycle and 11 MPa for 3 cycles. The mixes were cooled to 25 °C and aged at 4 °C overnight.

2.3. Ice cream preparation

Ice cream samples were made with two freezing methods to vary the overrun and ice crystal size. According to the first method, the ice cream mix (1 L) was frozen in a batch freezer (Frigomat T4S-T5S, Italy) for 10 min to a drawing temperature of approximately −10 °C. The overrun was measured after freezing and the obtained ice cream was collected into 250 ml containers and hardened at −20 °C for 24 h. According to the second method, the ice cream mix (1 L) was first whipped with a milk frother (KitchenSpecials, Netherlands) with a fixed speed for 2 min, after which the mix was poured into a Mixer (Bosch MFQ36460, Netherlands). Liquid nitrogen was gradually added during shearing to gradually decrease temperature. During the process, samples with a constant volume were taken to determine the weight of the ice cream and the corresponding overrun. Ice creams with varying overrun (30, 60 and 90%) were collected in plastic containers or rings of different sizes to form solid ice cream cylinders for different measurements and were hardened at −20 °C for 24 h. An overview of the studied ice cream samples is shown in Table 1. The samples are coded according to the process used (BF: batch freezer, LN: liquid nitrogen), overrun (30, 60 or 90%) and the emulsifier used (WPI or T80).

Table 1
Overview of the studied ice cream samples.

Series		Sample code
WPI series	Ice cream mix	MIX-WPI
	LN series	LN-90-WPI
		LN-60-WPI
		LN-30-WPI
	BF series	BF-30-WPI
T80 series	Ice cream mix	MIX-T80
	LN series	LN-90-T80
		LN-60-T80
		LN-30-T80
	BF series	BF-30-T80

2.4. Ice cream microstructure

2.4.1. Overrun

The overrun of ice cream pre-mix foam (whipped ice cream mix) and frozen ice cream was determined by first weighing a fixed volume of the aged pre-mix in a metal cup. Next, the same volume of either whipped ice cream mix or ice cream was weighted in the cup directly after whipping or ice cream preparation. The overrun was quantified as (Muse et al., 2004):

$$\text{Overrun } (\%) = \frac{\textit{Weight of mix} - \textit{weight of ice cream}}{\textit{Weight of ice cream}} \times 100 \quad (1)$$

2.4.2. Particle size distribution

The fat particle size distribution of the pre-mix and molten ice cream was measured with static light scattering (Mastersizer 2000, Malvern Instruments, Ltd, Malvern, Worcestershire, UK), using a refractive index of 1.46 and 1.33 for the fat and the water, respectively. The initial fat globule size was obtained from the peak of the pre-mix. From the bimodal distribution of the molten ice cream, we extracted two additional parameters, according to our previous work (Liu, Sala, & Scholten, 2022). The mean particle size of each individual peak ($D_{4,3}$) was determined separately, and the volume percentage of the second peak was used to reflect the degree of fat destabilization as fat aggregate percentage. Measurements were performed at room temperature and repeated in triplicate.

2.4.3. Ice crystal size

The analysis of ice crystal size was modified according to the method described by Velásquez-Cock et al. (2019). A light microscope with a hot stage (Zeiss Axioskop 2 Plus, Germany) was used to observe the ice crystals. The temperature of the hot stage was set at −20 °C, and all tools, reagents and samples were kept at −20 °C before the samples were prepared. Five mg of ice cream were taken from the core section of each container with a sharp knife and deposited over a standard glass slide. One or two drops of kerosene were applied to disperse the ice crystals more evenly, and the glass slide was covered with a chilled cover slide. The ice crystals were spread out gently by tapping the cover slide with chilled tweezers. The whole sample preparation process was carried out in a −20 °C storage room to prevent the melting of the ice crystals. The radius of the ice crystals was determined from these images assuming the ice crystals to have a spherical shape. A circle was placed around the ice crystals manually, from which the area and radius of the circle were determined by the software ZEN 2011. Ice crystal images were taken at 10x magnification to acquire at least 300 ice crystals to calculate the mean ice crystal radius and standard deviation of the samples.

2.4.4. Microstructure evaluation by X-Ray Tomography

To visualize differences in structure, two samples (LN-30-T80 and LN-90-T80) were evaluated with X-Ray Tomography (XRT). A cylindrically-shaped ice cream sample of 1.5–2 cm in height and 1 cm in diameter was extracted by pressing plastic tubes into the frozen ice cream. Samples were stored at −20 °C before measurements. An X-Ray Tomograph (GE phoenix v[tome] x m 240, United States) fitted with a nano-focus head and a 100 kV/10W transmission target was used to observe the three-dimensional structure of the frozen ice cream samples. A custom-made isolated sample holder equipped with an ice-filled bucket was cooled to −20 °C to keep the ice cream samples in a frozen state. The samples were loaded into the holder and scanned at 90 kV and 320 μA. Approximately 1800 projections were taken during a full rotation of 360° and the exposure time of each projection was 333 ms, with filtering turned off, and shift and auto scan optimizer enabled. The collected images were reconstructed into a three-dimensional representation using reconstruction software (GE Phoenix dataosx rec) with 1800 × 1800 × 1000 pixels. The mean size of the air cells and the thickness of the non-air phase were analyzed by Avizo 2019.4 after further processing.

2.5. Viscoelastic behavior, hardness and melting properties of ice cream

2.5.1. Oscillatory rheology

The rheological evaluation of frozen ice cream was performed with a Physica MCR 501 rheometer (Anton Paar, Germany), using a plate-plate geometry (PP50/P2). A moveable hood covering the plate-plate geometry was connected to the cooling system to control the temperature of the plate. An air pump was also connected to the hood to prevent heat exchange with the environment. Ice cream tablets (−20 °C) of 5 mm height and 25 mm diameter were taken out of the metal rings using a cylindrical cutting tool and were transferred to the plate (PP50) immediately. The initial force was set at 5 N to guarantee that the upper plate touched the sample tightly before starting the measurements. The gap width between the plates was adjusted to a constant value of 3 mm, which was small enough to keep contact between the probe and the sample during the entire duration of the measurements. Strain sweeps were carried out in a strain range from 0.0001 to 10%, at a frequency of 1.6 Hz (which was in the linear viscoelastic regime) and at a temperature of −10 °C to keep the ice cream at the frozen state. Storage modulus (G') and loss modulus (G") were measured and were plotted as a function of strain.

Temperature sweeps were used to characterize the melting process of studied ice cream with increasing temperature (−20 to 10 °C). Measurements were performed at a constant deformation of 0.005% and a frequency of 1.6 Hz with a plate-plate geometry (PP50/P2). Prior to the measurement, the temperature of the plate was reduced to −20 °C. The temperature was increased from −20 to 10 °C with a heating rate of 0.5 °C/min. Sixty measuring points were recorded with 1 min between measuring points. At least two measurements for each ice cream sample were carried out. G' and G" were plotted as a function of temperature.

2.5.2. Hardness

The hardness of the samples was measured with a Texture Analyzer (TA-TX plus, Stable Micro Systems, UK). Samples with the same volume were prepared using plastic rings. The dimensions of the samples were 25 mm in height and 60 mm in diameter. The samples were stored in a freezer at −20 °C for a minimum of 24 h. Prior to the measurement, a climate chamber was connected to the Texture Analyzer to maintain a temperature of −20 °C. The samples were taken out of the plastic rings using a cylindrical cutting tool and transferred to the climate chamber immediately. Then the samples were measured using an aluminum cylinder probe (10 mm in diameter) attached to a 50 kg load cell and were penetrated to a strain of 50% at a speed of 2 mm/s. Instrumental hardness was defined as the maximum peak force during penetration of each sample.

2.5.3. Melting test at room temperature

The melting properties of the samples were measured at room temperature (20 °C). Samples with the same volume were prepared using plastic rings with 25 mm height and 60 mm diameter. Prior to measurements, the samples were stored overnight in a freezer at −20 °C. Then the samples were taken out of the rings and placed on a 136 × 136 mm metal grid with 5 × 5 mm holes representing 44% of the total area of the metal grid. The starting weight of each sample was measured and a collection cup was placed on a measuring scale underneath the mesh. The weight of the molten sample was measured every 10 s, at a temperature of 20 °C, for a duration of 240 min. Three phases could be identified during the whole melting process: (i) a lag phase, (ii) a fast-melting phase, and (iii) a plateau phase. The lag phase corresponds to the phase until the first droplet dripped, from which the lag time (min) was obtained. The fast-melting phase corresponds to the phase between the end of the lag phase and the beginning of plateau phase, from which the melting rate (%/min) was determined from the slope. From the plateau phase, representing the phase after complete melting, the

melted percentage (%) was determined as the loss of total ice cream after complete melting. The measurements were performed in duplicate.

2.5.4. Statistical analysis

The data were analyzed by SPSS software (Version 25.0, IBM Corp). The means were compared using a Duncan's test at a 5% level of significance using the analysis of variance (ANOVA).

3. Results and discussion

3.1. Characteristics of the model ice cream samples

3.1.1. Variations in overrun

Variations in the overrun of the different samples were obtaining by applying different ice cream making procedures. In samples made with a batch freezer, the overrun increased within 3 min to around 30% (data not shown) and then remained constant with increasing freezing time (10 min). This method allowed to obtain ice cream with constant overrun. On the other hand, the liquid nitrogen freezing process optimized for our research allowed to obtain samples with varying overrun. According to this process, liquid nitrogen was added into pre-whipped ice cream mixes. The gradual addition led to a decrease in temperature from 4 to −4 °C with a much slower cooling rate, as a limited amount of liquid nitrogen was added at a time (the ratio liquid nitrogen: pre-mix was kept around 1:30). This process resulted in higher overrun values, and with increasing processing time these values gradually decreased. Specifically, the overrun decreased from 240 to 30% in the WPI series (Fig. 1a), while a less pronounced decrease, from 110 to 30%, was seen in the T80 series (Fig. 1b). The difference in the evolution of the overrun can be attributed to the different stability of the air cells. In the WPI series, the air cells were mainly stabilized by fat droplets and whey protein, while in the T80 series the air cells were stabilized by fat droplets, fat droplet aggregates and Tween 80. The higher ability of whey protein to stabilize air cells resulted in a higher initial overrun in the WPI series. As freezing proceeded, the air cells in the WPI series were progressively more destabilized and the overrun decreased. Although the initial overrun in the T80 series was lower, the aggregation of the fat droplets provided more stability to the air bubbles, and therefore the decrease in overrun was more limited. For both the WPI and T80 series, we could collect samples with different overrun (approximately 30, 60 and 90%) by sampling at different times during processing, as indicated in Fig. 1 with red circles. At the moment of collection, the ice content was different, but after the hardening step, it was the same in all samples, as the ratio sugar: water was kept the same.

3.1.2. XRT analysis for ice cream microstructure

To obtain information on the structural organization of the air cells and the non-air phase, we analyzed two representative ice cream samples with X-Ray Tomography. As this method relies on density differences between phases, we were only able to distinguish between the dispersed air phase and the non-air phase, but no information on the fat phase could be obtained. We selected a sample with 30% overrun and one with 90% overrun from the T80 series. The results are shown in Fig. 2. From the image reconstruction, the mean size of air cells and the mean distance between air cells (thickness of non-air phase) were quantified. The sample with low overrun was of course much denser, with a mean air cell size of 34 μm, and a mean thickness of the non-air (serum) phase between the air of 178 μm. For higher overrun (90%), the structure was more open, with a mean air cell size of 165 μm, and a much lower thickness of the non-air (serum) phase of 69 μm. Similar indications were reported by Koxholt, Eisenmann, and Hinrichs (2001), who showed that higher overrun leads to thinner lamellae between the air cells.

3.1.3. Variations in fat destabilization

The degree of fat destabilization in the WPI and T80 series was determined by measuring the fat particle size distribution of pre-mix and molten ice cream. As shown in Fig. 3, a bimodal distribution was found for both the WPI series (Fig. 3a) and the T80 series (Fig. 3b). The first peak (0.01–10 μm) corresponded to the single fat droplets, and the second peak to aggregated fat droplets with a size over 10 μm. From these results, two parameters were used to quantify the fat destabilization degree: (1) mean fat particle size ($D_{4,3}$), and (2) fat aggregate percentage (determined from the second peak), which are summarized in Table 2 for both series.

In the WPI series, limited fat destabilization took place, independently of the freezing process, and samples with different overruns also had similar particle size distribution (Fig. 3a). In the curves of Fig. 3, a small shoulder/peak with a mean size around 0.2 μm could be observed, which could be attributed to whey protein aggregates present in the continuous phase. As shown in Table 2, the particle size ranged from 1.4 to 2.6 μm, and the fat aggregate percentage was less than 3.9%. Comparatively, in the T80 series (Fig. 3b), a higher degree of fat destabilization was found for both freezing processes. This was expected, as it is known that small molecular weight emulsifiers (T80) provide less stability against aggregation compared to proteins, which tend to form a thicker and more viscoelastic membrane at the oil/water interface (Fredrick, Walstra, & Dewettinck, 2010). The mean fat particle size of the T80 ice creams made with liquid nitrogen ranged between 44 and 107 μm, and the percentage of fat aggregates ranged between 72 and 100%. This can be explained by the increasing processing time, as it has been found that the degree of fat destabilization in ice cream is influenced by shear forces and freezing time (Chang et al., 2002). Samples with higher overrun had a lower total freezing time, and

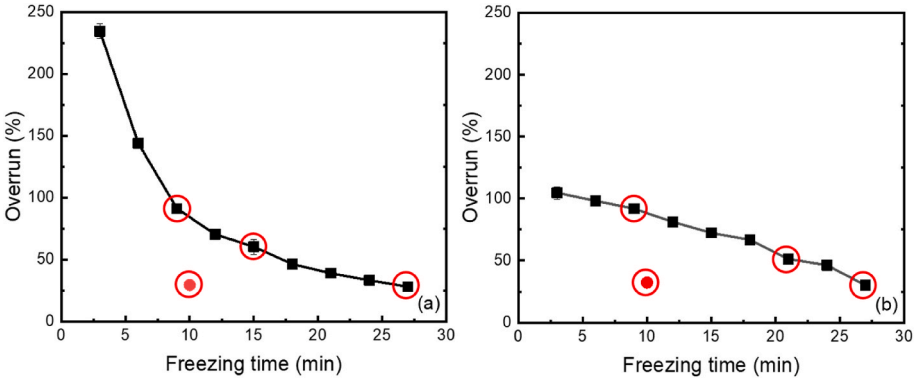

Fig. 1. Overrun changes in (a) WPI and (b) T80 ice cream series during freezing in a batch freezer (BF) and with liquid nitrogen (LN). LN: black squares, BF: red dot. The times of sample collection are highlighted with red circles. (For interpretation of the references to color in this figure legend, the reader is referred to the Web version of this article.)

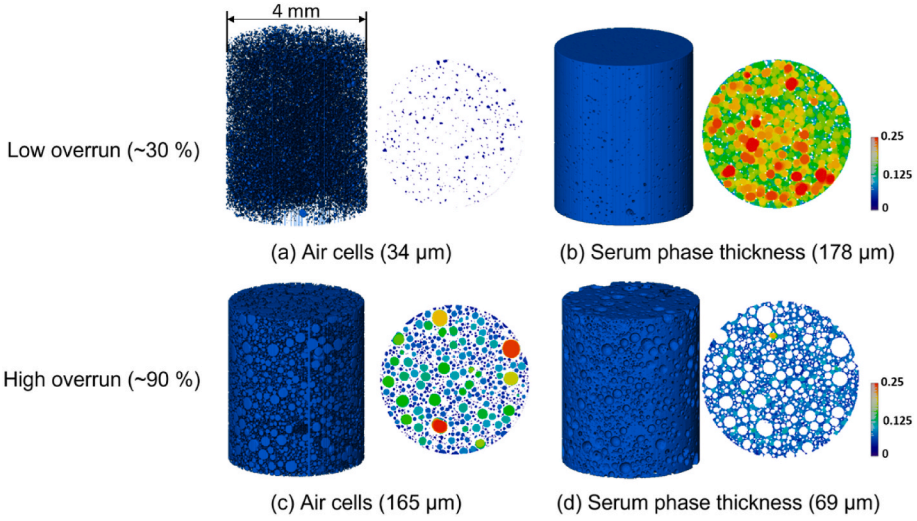

Fig. 2. Images of the 3D microstructure of ice creams with different overrun level from the T80 series. The air and non-air phase were examined for the mean size of the air cells, and the thickness of the (non-air) serum phase. The dimensions of the cylinders were 4.5 mm in height and 4 mm in diameter. The warmer (red) colors indicate higher values of air cell size or serum phase thickness and colder (blue) colors indicate lower values. (For interpretation of the references to color in this figure legend, the reader is referred to the Web version of this article.)

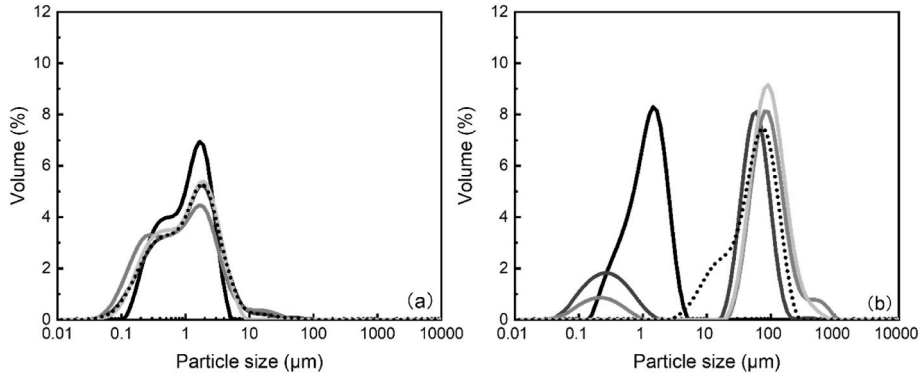

Fig. 3. Fat particle size distribution of the (a) WPI and (b) T80 ice cream series (including mix and molten ice cream). MIX: black line; LN-90: dark grey; LN-60: grey; LN-30: light grey; BF-30: black dotted line.

Table 2
Mean particle size and degree of fat destabilization of the WPI and T80 ice cream series.

Ingredients		Mean particle size, $D_{4,3}$ (μm)	Fat aggregate percentage (%)
WPI series	Mix	1.2 ± 0.1^{e}	0
	LN-90-WPI	2.6 ± 0.2^{e}	0
	LN-60-WPI	1.7 ± 0.1^{e}	3.1 ± 0.2^{e}
	LN-30-WPI	1.4 ± 0.1^{e}	3.9 ± 0.1^{e}
	BF-30-WPI	2.0 ± 0.1^{e}	2.4 ± 0.3^{ef}
T80 series	Mix	1.5 ± 0.1^{e}	0
	LN-90-T80	44 ± 2^{d}	72 ± 1^{d}
	LN-60-T80	85 ± 7^{b}	84 ± 2^{c}
	LN-30-T80	107 ± 9^{a}	100^{a}
	BF-30-T80	62 ± 1^{c}	94 ± 1^{b}

Values with a different letter within the same column are significantly different ($P < 0.05$).

showed therefore a lower degree of fat destabilization. In addition, in the T80 ice cream samples prepared with the batch freezer and low overrun (BF-30-T80), the $D_{4,3}$ and the percentage of fat aggregates were 62 μm and 94%, respectively. These values were relatively low compared with those of the liquid nitrogen ice cream sample at the same overrun level (LN-30-T80), which were 107 μm and 100%. This difference can also be attributed to the longer freezing time with the liquid nitrogen freezing process. Thus, both the emulsifier type and freezing time were used to control the degree of fat destabilization.

3.1.4. Ice crystal size

The ice crystal size of the samples was expected to mainly be influenced by the freezing process. In fact, as shown in Table 3, for the WPI series, the average crystal radius was 22 μm for samples made with the batch freezer (BF-WPI), and approximately 41 μm for samples made with liquid nitrogen (LN-WPI), regardless of the overrun. For the T80 series, the ice crystal radii of samples made with the batch freezer (BF-T80) and liquid nitrogen (LN-T80) were 29 and 52 μm, respectively. For both series, the liquid nitrogen freezing process resulted in larger ice crystals than the batch freezer. These results were in contradiction with a previous study, in which liquid nitrogen provided smaller ice crystals (Goff & Hartel, 2013). These differences can be explained by the cooling rate. Although liquid nitrogen can lead to fast ice crystal nucleation due

Table 3
Mean radius of the ice crystals in the T80 and WPI ice cream series.

Ingredients		Ice crystal radius (μm)
WPI series	LN-90-WPI	39 ± 6^{abc}
	LN-60-WPI	41 ± 9^{abc}
	LN-30-WPI	42 ± 6^{abc}
	BF-30-WPI	22 ± 6^{c}
T80 series	LN-90-T80	47 ± 12^{ab}
	LN-60-T80	52 ± 6^{a}
	LN-30-T80	57 ± 13^{a}
	BF-30-T80	29 ± 7^{bc}

Values with a different letter within the same column are significantly different ($P < 0.05$).

to its very low temperature, the cooling rate is actually determined by the ratio between pre-mix and liquid nitrogen. As we only added a very limited amount of liquid nitrogen at a time, the cooling rate was much lower than that in the batch freezer. A lower cooling rate thus resulted in larger ice crystals. In addition, the longer freezing time could be another reason for the inconsistency between our results and those of Goff and Hartel (2013), as a longer processing time has been shown to produce ice creams with larger ice crystals due to the greater extent of recrystallization (Drewett & Hartel, 2007; Russell et al., 1999).

Some differences in ice crystal size could also be found between the T80 and the WPI series. Ice cream of the latter series (Fig. 4a) showed small ice crystals, whereas the T80 series contained slightly larger ice crystals (Fig. 4b). As the ice faction was the same in all studied samples, the number of ice crystals was higher in samples with smaller ice crystals. This most probably led to a higher ice connectivity in the WPI samples. As in the T80 series a fat network was formed by destabilized fat aggregates, we could also speculate that the contact frequency among ice crystals was reduced, resulting in lower ice connectivity and larger ice crystals. Therefore, samples with WPI had smaller ice crystals with higher ice connectivity, whereas T80 samples had large ice crystals with low ice connectivity. These results showed that in our samples, next to overrun and fat destabilization degree, also ice crystal size could in fact be controlled.

3.1.5. Dominating structure in the two series

To get insights in the dominating structures present in the studied samples, we examined their shape retention after melting for 3 h, which is related to the formation of a fat network remaining behind at the end of the melting process (Liu et al., 2022). As shown in Fig. 5, a significant difference in shape retention could be found between the two series. The samples of the WPI series presented a low ability to retain their structure due to a limited degree of fat destabilization, while the samples of the T80 series showed strong shape retention after melting. As both series had the same fat content, we can conclude that the main reason leading to the different shape retention was the different degree of fat destabilization, which resulted in a significantly different microstructure in the two series.

Based on the results presented above, in Fig. 6 we propose a schematic representation of the microstructure of the WPI and T80 ice creams. In the case of the WPI series, the dominant structure was formed by the ice crystals due to the limited degree of fat destabilization. The ice crystal structure was formed by the smaller ice crystals and a higher ice connectivity between the smaller crystals (Fig. 6a). In comparison, in the case of the T80 series, a high degree of fat destabilization resulted in a fat network-dominated structure, in which ice crystals and air cells acted as fillers (Fig. 6b). Thus, at the same fat content and ice fraction, ice creams with two significant different microstructures were identified, by which we could clarify the separate contribution of fat network, overrun and ice crystal size.

3.2. Viscoelastic behavior, hardness and melting properties of the two model ice cream series

3.2.1. Effect of structure on viscoelastic behavior

Using different ingredients and freezing processes, we were able to control the different microstructural elements of our samples. To unveil how their intrinsic arrangement and the interactions among them affected the viscoelastic behavior of the ice cream, we measured G' and G" as a function of the applied strain (Fig. 7). To gain insights in the role of the fat network, we compared BF-30-WPI (black circles) and BF-30-T80 (grey circles), which had a similar ice crystal size ($P > 0.05$) and the same overrun (30%), but a different fat destabilization degree (Fig. 7a). BF-30-WPI, the sample with a lower degree of fat destabilization, showed a longer linear viscoelastic regime (LVR) than BF-30-T80. In addition, although the G' and G" were similar at low strain (lower than 0.002%), they decreased less with increasing strain for BF-30-WPI than for BF-30-T80. The difference can be explained by the difference in the dominating contribution. The sample with a higher contribution of the ice crystal structure and the weaker fat network (BF-30-WPI) presented the most solid like properties (higher G') upon increasing deformation.

To clarify the effect of ice crystal size on the viscoelastic behavior of the WPI series, we compared the moduli of LN-30-WPI (black squares) and BF-30-WPI (black circles), which had similar limited degree of fat destabilization and overrun (30%), but a different ice crystal size (42 and 22 μm). As shown in Fig. 7b, within the whole strain range, similar G' and G" could be found for both samples. The solid-like properties were thus more determined by the total ice content, and the ice crystal size or connectivity had limited effect. A similar trend could also be found in the T80 series (Fig. S1a in supplementary material): the sample LN-30-T80 with larger ice crystal size and a higher degree of fat destabilization showed similar G' and G" as BF-30-T80 within the whole strain range. The fat aggregates could reduce the connectivity of the ice crystals even further, but the differences between the samples were limited.

In addition, by comparing the viscoelastic behavior of LN-30-WPI (black squares) and LN-90-WPI (light grey squares), which had a similar ice crystal size (approximately 40 μm) and degree of fat destabilization, but a different overrun of 30 and 90%, respectively, the effect of overrun on the viscoelastic properties could be identified. As can be seen from Fig. 7c, within the whole strain range, LN-30-WPI showed higher values of G' and G" than LN-90-WPI. The higher moduli for samples with lower overrun could be attributed to the formation of a more connected ice crystal structure in the LN-30-WPI sample. Ice cream with a lower overrun was expected to have a thicker serum phase, which would lead to more contacts among ice crystals. Similarly, LN-30-T80, with lower overrun but higher degree of fat destabilization, also showed higher values of G' and G" than LN-90-T80 within the whole strain range, but the differences between these two samples decreased with increasing strain (Fig. S1b supplementary material). The smaller

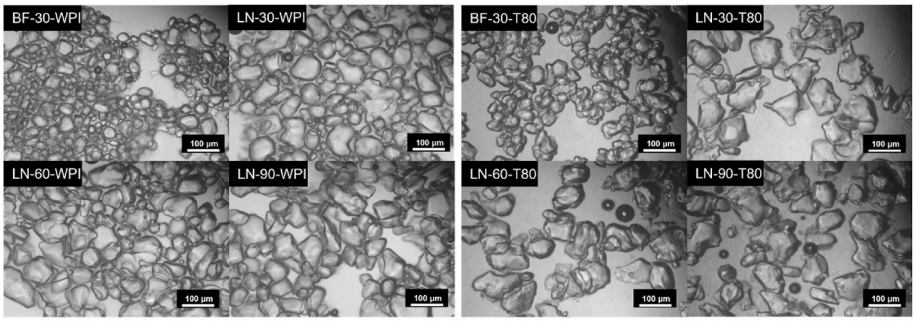

Fig. 4. Images of ice crystals in the (a) WPI and (b) T80 ice cream series. Top left: samples prepared with a batch freezer (BF). Top right: samples made with liquid nitrogen (LN) with an overrun of 30%. Bottom: samples made with LN with 60% (left) and 90% (right) overrun.

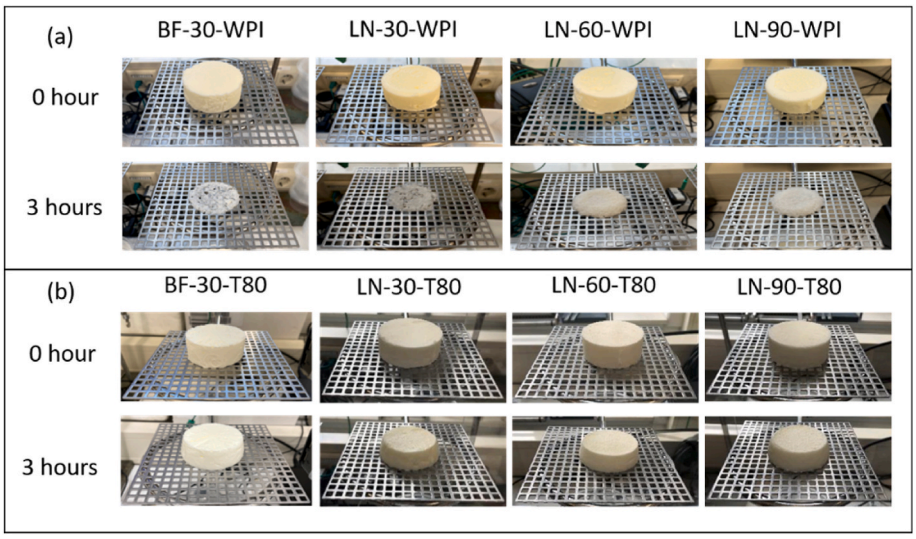

Fig. 5. Shape retention of the (a) WPI and (b) T80 ice cream series after 3 h melting at 20 °C. From left to right: samples prepared with the batch freezer (BF) with 30% overrun, and samples prepared with liquid nitrogen (LN) with 30%, 60% and 90% overrun.

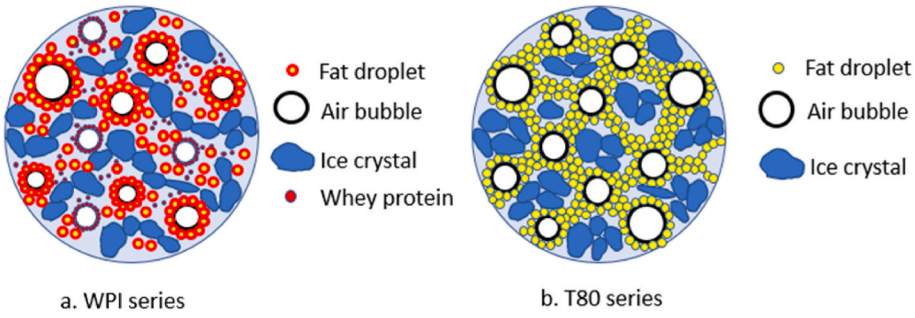

Fig. 6. Schematic representation of the (a) ice crystal-dominated structure (WPI series) and (b) fat network-dominated structure (T80 series). This figure is not drawn to scale.

difference between G' and G" can be explained by the effect of the fat network on the ice crystal-dominated structure. The sample with a higher overrun had a lower degree of fat destabilization and thus a weaker fat network, which had a lower influence on ice crystal connectivity. Therefore, the difference in the connectivity between the ice crystals between low and high overrun samples was smaller. As discussed above, the viscoelastic properties of ice cream were dominated by the ice crystal structure, and, therefore, a smaller difference between G' and G" was expected between LN-30-T80 and LN-90-T80 (Fig. S1b supplementary material), as both samples have a fat-dominated network. The effect of rheological and structural components (mix viscosity, overrun and fat destabilization) on the viscoelastic properties of ice cream was also reported by Freire, Wu, and Hartel (2020). In this article, $G'_{-15^{\circ}C}$ was used to characterize the viscoelastic properties of the ice cream. In this paper, $G'_{-15^{\circ}C}$ was strongly correlated with mix viscosity, but did not appear to significantly relate to overrun and fat destabilization. An inverse correlation was found between mix viscosity and $G'_{-15^{\circ}C}$, and the authors attributed this to a loss in connectivity among ice crystals as a result of the presence of a serum phase in which the polysaccharides were highly entangled (as result of freeze concentration of the serum phase). Due to the high viscosity of their samples, they did not see any effects of overrun and fat destabilization. However, when the effect of viscosity is reduced, which is the case in our study, a clear inverse correlation can be observed between overrun and G' in both the ice crystal-dominated and fat network-dominated series. As discussed above, this can be explained by a loss in connectivity among ice crystals due to high overrun values. In addition, although no clear effect of fat destabilization on G' and G" could be found within the LVR, we could observe that fat destabilization had a negative effect on the G' and G" with increasing strain, clarifying that fat destabilization mainly plays a role upon large deformation.

In conclusion, the viscoelastic properties of ice cream were mainly determined by the ice crystal structure. The effect of ice crystal size on the viscoelastic behavior of both series was limited. However, the overrun had a larger effect on the viscoelastic moduli of samples with an ice crystal-dominated structure, due to a secondary effect of the influence of the fat network on the connectivity between ice crystals. Increasing overrun weakened the structure of ice crystals and thus led to lower viscoelastic moduli. Although oscillatory rheology has not been extensively used in ice cream research, our results showed that this technique can provide valuable information on the structural organization of this food.

3.2.2. *Hardness*

As evidenced with oscillatory shear experiments, the different structural elements of the samples affected the strength of the structure and the resistance against collapse after melting of the ice fraction. The ice crystal-dominated structure was shown to contribute the most to the solid-like behavior, and was thus expected to strongly influence also the hardness of the ice cream. The hardness of both the WPI and the T80 series was determined by performing penetration tests. As shown in Fig. 8, in both series, samples with smaller ice crystals (BF samples, dark grey) had hardness similar ($P > 0.05$) to that of samples with the same overrun but larger ice crystals (LN-30, black), indicating that ice crystal

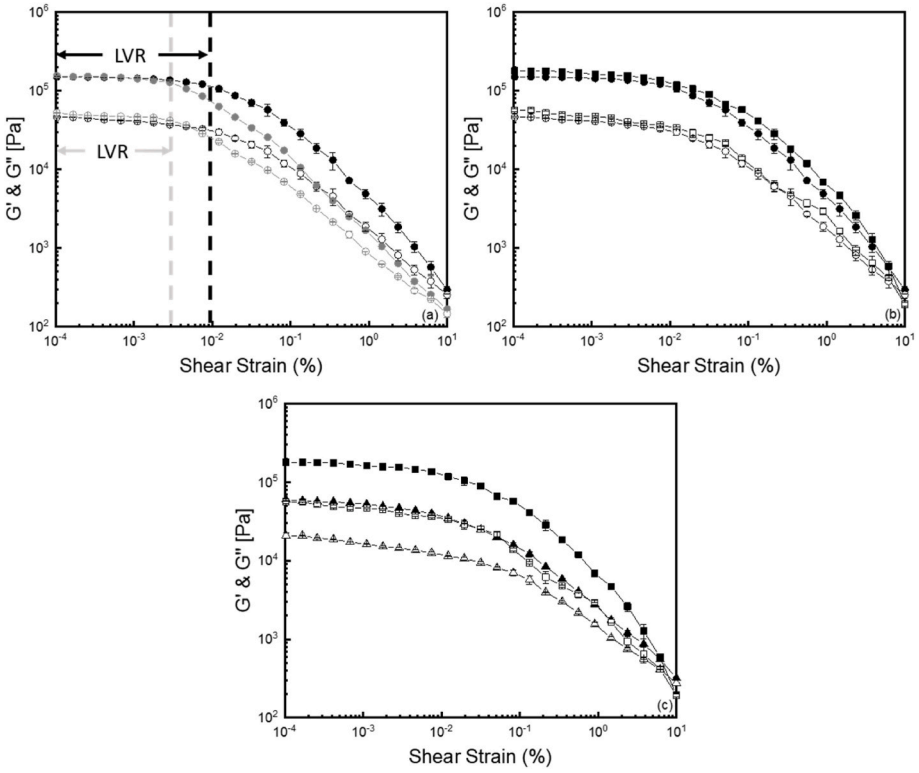

Fig. 7. Storage modulus (G') and loss modulus (G") as a function of strain for samples with different structural elements. (a) Samples with varying fat destabilization degree: BF-30-WPI (black circles) and BF-30-T80 (grey circles); (b) samples with varying ice crystal size: LN-30-WPI (black squares) and BF-30-WPI (black circles); (c) samples with varying overrun: LN-30-WPI (black squares), and LN-90-WPI (black triangles). G' is provided as solid symbols, and G" as empty symbols. WPI series are shown as black color, and T80 series as grey color.

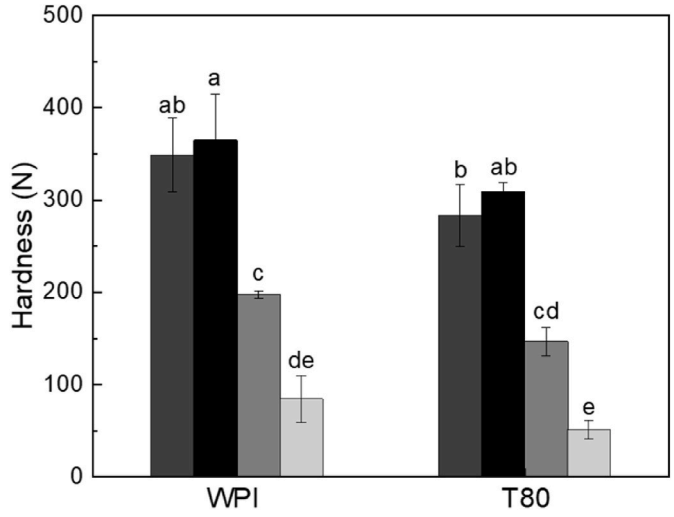

Fig. 8. Hardness of the WPI and T80 ice cream series. BF-30-WPI and BF-30-T80 (dark grey), LN-30-WPI and LN-30-T80 (black), LN-60-WPI and LN-60-T80 (grey), LN-90-WPI and LN-90-T80 (light grey). Values with a different letter above the bars are significantly different ($P < 0.05$).

size did not affect hardness. The connectivity among ice crystals, therefore, does not seem to affect ice cream structure at large deformation.

A clear effect of overrun was observed in Fig. 8. For both the WPI and T80 series, the lowest hardness was observed in high overrun ice creams (90%, light grey bars), and its value increased when the overrun decreased (30%, black bars). This relationship has been reported by many researchers (Biasutti, Venir, Marino, Maifreni, & Innocente, 2013; das Graças Pereira, de Resende, de Abreu, de Oliveira Giarola, & Perrone, 2011; Syed, Anwar, Shukat, & Zahoor, 2018). Limited differences were observed between the WPI and T80 series, indicating that the type of dominated structure had a negligible effect on hardness. In both ice crystal-dominated and fat network-dominated structures, the effect of overrun on hardness was similar, by limiting the formation of either structure. In spite of this, we did see some effect of fat destabilization on hardness. Samples with a higher fat destabilization degree (T80 samples) and with similar overruns had a slightly lower hardness than samples without fat destabilization (WPI series). This could be attributed to the fact that the fat network (T80 samples) was less solid compared with the ice crystal-dominated structure. In addition, a higher degree of fat destabilization could limit the formation of an ice crystal-dominated structure even further. The lower connectivity between ice crystals in T80 samples thus led to reduced hardness. This finding is consistent with the results found with oscillatory shear experiments, in which higher moduli were found with increasing strain in samples with a more extended ice crystal-dominated structure (WPI samples). Therefore, it can be concluded that the ice crystal-dominated structure plays a major role in determining hardness.

3.2.3. *Structure changes during melting*

The results discussed above show that in our samples the ice crystal structure had the largest effect on hardness. The effect of the microstructure during melting was also evaluated by measuring G' and G" as a function of temperature. Fig. 9 shows the structural changes of ice creams with either an ice crystal-dominated (BF-30-WPI) or a fat network-dominated (BF-30-T80) structure. All measurements were carried out within the LVR, and in the obtained curves three zones can be identified; (1) zone I, from −20 to −3 °C: in this temperature range the solid behavior of the sample dominates the rheological properties as the ice cream is still in its frozen state; (2) zone II, between −3 and 4 °C: in this region, the moduli show a steep decrease, which indicates the fast-melting state of the ice cream; (3) zone III, from 4 to 10 °C: within this zone, the rheological behavior of ice cream is dominated by the microstructure of the molten ice cream (Eisner, Wildmoser, & Windhab, 2005).

As shown in Fig. 9, in zone I, similar G' and G" were observed for the ice creams with different degrees of fat destabilization, indicating that

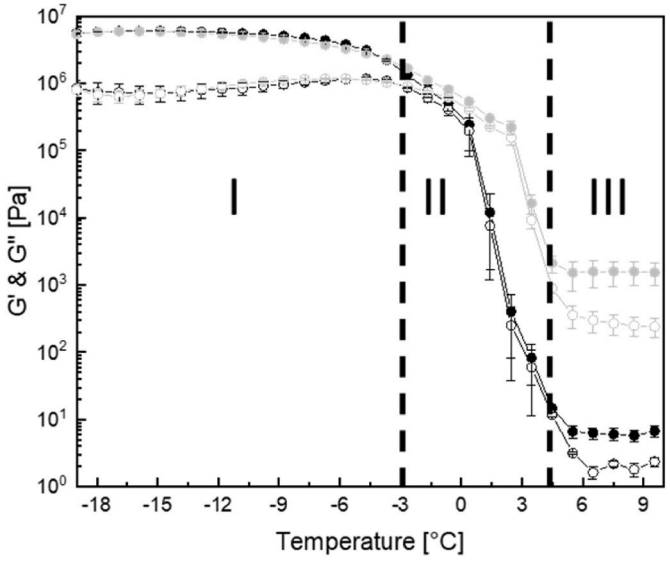

Fig. 9. Storage modulus (G') and loss modulus (G") as a function of temperature for samples with two different structures as a result of different fat destabilization degree. Ice crystal-dominated structure: BF-30-WPI (black circles); fat network-dominated structure, BF-30-T80 (grey circles). G' is provided as solid symbols, and G" as empty symbols.

ice crystals and a fat network had a similar contribution to the viscoelastic properties at small deformation. This result was consistent with the data from the strain sweep within the LVR (Fig. 7a). Although in the frozen state the effect of microstructure was limited, larger effects were seen in the fast-melting state (zone II). A fast and early decrease of both G' and G" was seen for the sample dominated by an ice crystal structure (black symbols). However, for samples dominated by a fat network, the decrease in G' and G" occurred mainly at higher temperature, which corresponded to a slower melting. This result indicated that the formation of a fat network had a significant influence on the melting process. In addition, the fat network was also able to entrap the serum phase, which was reflected by the relatively lower melting rate and melted percentage (Fig. 5). As a matter of fact, when fat droplets are present as a 3D network, drainage of the serum phase is prevented. This result is in agreement with studies by other authors (Warren et al., 2014; 2018). In zone III, all samples melted completely. Due to the 3D network of fat particles, G' and G" were still high in samples with a fat network dominated structure, whereas samples with an ice crystal-dominated structure showed much lower G' and G", as limited fat destabilization was present.

To clarify the effect of ice crystal size on structure changes during melting, we compared samples of both the WPI (Fig. 10a) and T80 series (Fig. 10b) with a low overrun of 30%, prepared with either a batch freezer (BF) or liquid nitrogen (LN), and thus with different ice crystal size. As shown in Fig. 10a, for WPI samples, similar G' and G" were observed in ice creams with different ice crystal size in all three zones. These results showed that ice crystal size did not have a significant influence on the melting process. As also concluded from the results of the oscillatory shear experiments, the structure of the ice crystals was dominated by ice content, and ice crystal size had limited influence. Also for the T80 samples (Fig. 10b), where the fat network was more prominent, similar G' and G" were found. However, at higher temperatures, differences in G' and G" started to appear, especially in zone III. Higher values were found for samples with larger ice crystals. This could be attributed to the fact that the fat aggregate percentage was also higher in the sample with a larger ice crystal size. As the ice crystals melted, the 3D fat network slowed down the melting process. Due to the disappearance of the ice crystals and their connectivity, the contribution of the fat network became more relevant.

The effect of overrun could be clarified by comparing samples with different overrun (30% and 90%) in both the ice crystal- and fat network-dominated series. As shown in Fig. 10c, for WPI samples with higher overrun (triangles), lower values for G' and G" were observed in zone I. As discussed in section 3.1.4, the overrun significantly influenced the thickness of the lamellae between air cells: a higher overrun corresponded to larger air cell size, leading to thinner lamellae. This

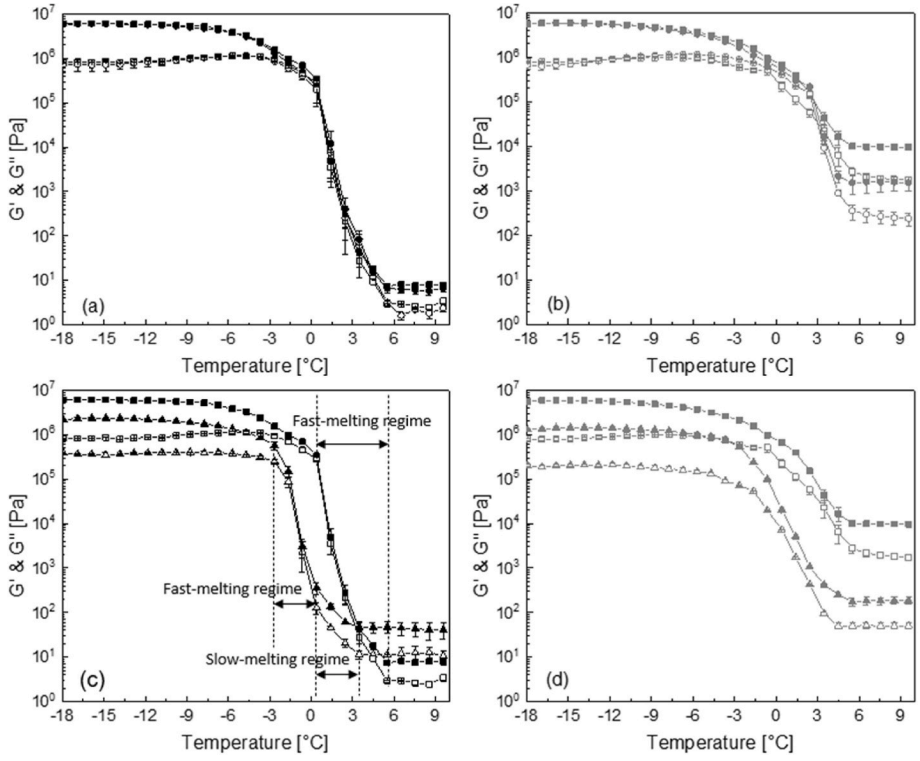

Fig. 10. Storage modulus (G') and loss modulus (G") as a function of temperature for samples with different structural elements. Samples with varying ice crystal size; (a) WPI series: LN-30-WPI (black squares) and BF-30-WPI (black circles) and (b) T80 series: LN-30-T80 (grey squares) and BF-30-T80 (grey circles). Sample with varying overrun; (c) WPI series: LN-30-WPI (black squares), and LN-90-WPI (black triangles), and (d) T80 series: LN-30-T80 (grey squares) and LN-90-T80 (grey triangles). G' is provided as solid symbols, and G" as empty symbols.

negatively affected the connectivity among ice crystals, which explained the lower values of the moduli. Due to the lower connectivity between the ice crystals, the moduli also started to decrease at a lower temperature, i.e. melting started earlier. However, at higher temperature, the melting slowed down, and therefore, two different melting regimes (fast-melting and slow-melting regime) were seen in zone II for the sample with high overrun. The low overrun sample (squares) showed only one fast-melting regime, but the melting started later (higher temperature). Although many results in literature claim that air is a good insulator and slows down the rate of heat transfer to the ice cream (Sofjan et al., 2004; Wu, Freire, & Hartel, 2019), our results clarified that the structure obtained by the ice crystals seems to be more important for initial melting than the overrun, and that the overrun mainly slows down melting at a later stage. The differences between our results and those of other authors concerning the effect of overrun on melting may be explained by differences in serum phase viscosity. In studies of other authors, polysaccharides were often added to the recipe and thus led to a high serum phase viscosity, which could stabilize the air cells during the melting process. However, in our study, no polysaccharides were used. The lower serum phase viscosity provided lower stability to the air cells, leading to a faster escape once the structure determined by the ice crystals collapsed. In the T80 series with a fat network-dominated structure, only one melting regime was found in zone II (Fig. 10d) and the melting was much slower. This again shows that the fat network had a strong influence on the melting rate. In these samples, overrun had a larger effect. The sample with higher overrun (triangles) started to melt at lower temperature and faster (higher slope of moduli curves). The faster melting is consistent with the samples of the WPI series, and contradicts the findings by others. For example, Warren et al. (2018) showed that ice creams with high overrun had a good melting resistance, due to the good insulating properties of air. These results show that not only the overrun is important, but that the network or structure in which the air is incorporated plays a larger role. In the study of Warren, the sample with higher overrun also corresponded with a higher level of fat partial coalescence. However, in our case, a lower degree of fat destabilization was found in the high overrun sample. As shown in Fig. 2, the thickness of the lamellae between air cells was 178 μm for the low overrun sample, and 69 μm for the high overrun sample, and the fat aggregate size was 107 and 44 μm, respectively (Table 2). These results show that the stronger fat network in the thicker serum phase had a higher ability to resist melting, even though these samples have a lower overrun. The effect of air is thus very much dependent on the specific structure of the sample. In zone III, higher values of G' and G" were found for the high overrun WPI sample, indicating the air cells were able to provide some structural integrity when molten. However, higher values were found for the T80 samples with lower overrun, as it had a stronger fat network.

3.3. Melting properties

We also measured the melting properties of the different ice creams using a common test carried out at room temperature during which three melting parameters were determined: melting rate, lag time, and melted percentage of ice cream. The results are summarized in Table 4.

Ice crystal-dominated samples (WPI series) exhibited a significantly different melting behavior than fat network-dominated samples (T80 series). As shown in Table 4, for the fat network-dominated series, longer lag time, lower melting rate and lower melted percentage were found compared to the samples in which ice crystals were more dominant ($P < 0.05$). These results were consistent with the melting behavior obtained from temperature sweep measurements, where samples of the T80 series showed a higher initial temperature and a lower melting rate. This confirmed that in our sample a fat network played a larger role in affecting the melting process than the structure obtained by the ice crystals.

In the WPI series, dominated by the structure of ice crystals, ice crystal size (comparing LN-30-WPI and BF-30-WPI) did not appear to have a significant effect on melting rate, lag time and melted percentage ($P > 0.05$). These results were consistent with the observations in zone II in Fig. 10a, and contradict those obtained by Muse et al. (2004), who reported that the melting rate increased as ice crystal size increased. However, in their study, these samples varied also in degree of fat destabilization and overrun, making it difficult to draw firm conclusions on the role of ice crystal size. In our samples, only ice crystal size varied, and therefore, a direct link with the melting behavior could be made. Our results show that ice crystal size itself has limited influence, and that the structure obtained by the ice crystals or fat network plays a more important role. The limited influence of ice crystal size was also seen in the T80 series, where lag time and melting percentage ($P > 0.05$) for sample LN-30-T80 and BF-30-T80 were similar. However, a small effect of ice crystal size on melting rate was observed. We propose that this was an indirect effect of difference in the fat network.

Table 4
Overview of melting parameters of ice creams in WPI and T80 series.

Samples		Lag time (min)	Melting rate (%/min)	Melted percentage (%)
WPI series	LN-90-WPI	12.2 ± 1.7^{d}	2.3 ± 0.3^{a}	97.6 ± 2.0^{a}
	LN-60-WPI	12.8 ± 2.1^{d}	2.3 ± 0.1^{a}	98.4 ± 0.9^{a}
	LN-30-WPI	16.2 ± 0.7^{c}	2.2 ± 0.1^{a}	99.2 ± 0.6^{a}
	BF-30-WPI	17.9 ± 1.8^{c}	2.1 ± 0.1^{a}	98.0 ± 0.4^{a}
T80 series	LN-90-T80	18.0 ± 0.2^{c}	1.2 ± 0.2^{b}	40.6 ± 1.0^{c}
	LN-60-T80	23.2 ± 0.9^{b}	1.0 ± 0.1^{bc}	41.2 ± 1.8^{c}
	LN-30-T80	29.4 ± 1.3^{a}	0.7 ± 0.1^{c}	44.8 ± 0.5^{b}
	BF-30-T80	29.9 ± 0.8^{a}	1.1 ± 0.1^{b}	46.7 ± 1.2^{b}

Values with a different letter within the same column are significantly different ($P < 0.05$).

The overrun had a larger effect on the melting properties. In ice crystal-dominated systems, by comparing LN-90-WPI and LN-30-WPI, it could be concluded that increasing overrun decreased the lag time from 16.2 to 12.2 min. This result was in line with the findings in zone II in Fig. 10c. As discussed before, the lower lag time could be attributed to a lower connectivity between ice crystals. These results thus confirmed that in our samples the ice crystal-dominated structure was more important than the overrun for the start of the melting process, even though overrun has always been claimed to slow down melting. However, samples with different overrun showed similar melting rate and melted percentage, which seemed to be inconsistent with the observations in Fig. 10c. This was probably due to the different conditions during the melting process. When ice cream melts on a mesh screen, air cells can easily escape due to the collapse of the structure obtained by connecting ice crystals. However, during rheology measurements, the structure is more confined, leading to a slow-melting regime in Fig. 10c. For fat network-dominated systems, the effect of overrun was more pronounced. For samples with higher overrun (LN-90-T80), lag time decreased and melting rate increased. These results were consistent with the observations in Fig. 10d. A stronger fat network formed in the sample with a lower overrun (LN-30-T80) significantly delayed the melting process, which confirmed that the fat network is more important than overrun in resisting the melting.

By combining data obtained on a mesh screen with those derived from temperature sweeps, we could conclude that the presence of a fat network played a dominant role in determining the melting behavior. For fat network-dominated ice cream, all melting parameters were determined by the degree of fat destabilization, and overrun played a limited role. For ice crystal-dominated ice cream, the ice crystal structure was also more important than the overrun, but only at an early melting stage. At later stages when the structure of connecting ice crystals disappeared, the overrun could slow down the melting if air cells were well stabilized.

4. Conclusion

In this study, the role of fat destabilization degree, overrun and ice crystal size in determining the viscoelastic behavior, hardness and melting properties of ice cream was investigated. The structural factors were altered independently, which allowed us to extract the role of the individual factors. Due to differences in fat destabilization, ice creams with two significantly different microstructures were identified: an ice crystal-dominated structure and a fat network-dominated structure. For the ice crystal-dominated ice cream, changing ice crystal size had limited influence on viscoelastic moduli, hardness and melting behavior. Increasing overrun induced a loss of connectivity between ice crystals and thus led to lower viscoelastic moduli and hardness. The lower connectivity between ice crystals also caused earlier melting of the ice cream in the initial melting stage. At later stages of melting, higher overrun was able to slow down the melting process, leading to a two-step melting process. The ice crystal-dominated structure was shown to contribute more than the fat network to the solid-like properties of ice cream. For fat network-dominated structures, ice crystal size had limited effect. Overrun did affect hardness, but to a lesser extent than for the ice crystal-dominated samples. However, the fat network played a more dominant role in the melting properties. As a higher overrun disrupted the fat network, higher values of this parameter led to faster melting, even though overrun is generally assumed to slow down melting. These results revealed that the effect of the fat network on the melting behavior was more prominent than the effect of overrun.

CRediT authorship contribution statement

Xiangyu Liu: Investigation, Data curation, Methodology, Visualization, Writing – original draft. **Guido Sala:** Methodology, Conceptualization, Supervision, Writing – review & editing, Funding acquisition. **Elke Scholten:** Methodology, Conceptualization, Supervision, Writing – review & editing, Funding acquisition.

Declaration of competing interest

The authors declare that no competing interest exists.

Data availability

Data will be made available on request.

Acknowledgements

We appreciate the funding from Chicecream (Shanghai, China) and the China Scholarship Council (CSC NO. 201906330088). We thank Remco Hamoen for technical support of XRT measurements, performed on X-Ray Tomography equipment owned by Shared Research Facilities of WUR, and subsidized by the Ministry of Economic Affairs and the province of Gelderland, The Netherlands.

Appendix A. Supplementary data

Supplementary data to this article can be found online at https://doi.org/10.1016/j.foodhyd.2023.108466.

References

Amador, J., Hartel, R., & Rankin, S. (2017). The effects of fat structures and ice cream mix viscosity on physical and sensory properties of ice cream. *Journal of Food Science, 82*(8), 1851–1860.
Biasutti, M., Venir, E., Marino, M., Maifreni, M., & Innocente, N. (2013). Effects of high pressure homogenisation of ice cream mix on the physical and structural properties of ice cream. *International Dairy Journal, 32*(1), 40–45.
Chang, Y., & Hartel, R. W. (2002). Development of air cells in a batch ice cream freezer. *Journal of Food Engineering, 55*(1), 71–78.
Drewett, E. M., & Hartel, R. W. (2007). Ice crystallization in a scraped surface freezer. *Journal of Food Engineering, 78*(3), 1060–1066.
Eisner, M. D., Wildmoser, H., & Windhab, E. J. (2005). Air cell microstructuring in a high viscous ice cream matrix. *Colloids and Surfaces A: Physicochemical and Engineering Aspects, 263*(1–3), 390–399.
Fredrick, E., Walstra, P., & Dewettinck, K. (2010). Factors governing partial coalescence in oil-in-water emulsions. *Advances in Colloid and Interface Science, 153*(1–2), 30–42.
Freire, D. O., Wu, B., & Hartel, R. W. (2020). Effects of structural attributes on the rheological properties of ice cream and melted ice cream. *Journal of Food Science, 85*(11), 3885–3898.
Goff, H. D., & Hartel, R. W. (2013). *Ice cream.* Springer Science & Business Media.
Goff, H. D., & Jordan, W. K. (1989). Action of emulsifers in promoting fat destabilization during the manufacture of ice cream. *Journal of Dairy Science, 72*(1), 18–29.
das Graças Pereira, G., de Resende, J. V., de Abreu, L. R., de Oliveira Giarola, T. M., & Perrone, I. T. (2011). Influence of the partial substitution of skim milk powder for soy extract on ice cream structure and quality. *European Food Research and Technology, 232*(6), 1093–1102.
Koxholt, M. M. R., Eisenmann, B., & Hinrichs, J. (2001). Effect of the fat globule sizes on the meltdown of ice cream. *Journal of Dairy Science, 84*(1), 31–37.
Liu, X., Sala, G., & Scholten, E. (2022). Effect of fat aggregate size and percentage on the melting properties of ice cream. *Food Research International*, Article 111709.
Muse, M. R., & Hartel, R. W. (2004). Ice cream structural elements that affect melting rate and hardness. *Journal of Dairy Science, 87*(1), 1–10.
Prindiville, E. A., Marshall, R. T., & Heymann, H. (1999). Effect of milk fat on the sensory properties of chocolate ice cream. *Journal of Dairy Science, 82*(7), 1425–1432.
Russell, A. B., Cheney, P. E., & Wantling, S. D. (1999). Influence of freezing conditions on ice crystallisation in ice cream. *Journal of Food Engineering, 39*(2), 179–191.
Sakurai, K. (1996). Effect of production conditions on ice cream melting resistance and hardness. *Milchwissenschaft, 51*, 451–454.
Sofjan, R. P., & Hartel, R. W. (2004). Effects of overrun on structural and physical characteristics of ice cream. *International Dairy Journal, 14*(3), 255–262.
Syed, Q. A., Anwar, S., Shukat, R., & Zahoor, T. (2018). Effects of different ingredients on texture of ice cream. *Journal of Nutritional Health & Food Engineering, 8*(6), 422–435.
Tharp, B. W., Forrest, B., Swan, C., Dunning, L., & Hilmoe, M. (1998). Basic factors affecting ice cream meltdown. *International Dairy Federation Special Issue*, (3), 54–64.
Velásquez-Cock, J., Serpa, A., Vélez, L., Gañán, P., Hoyos, C. G., Castro, C., et al. (2019). Influence of cellulose nanofibrils on the structural elements of ice cream. *Food Hydrocolloids, 87*, 204–213.
Warren, M. M., & Hartel, R. W. (2014). Structural, compositional, and sensorial properties of United States commercial ice cream products. *Journal of Food Science, 79*(10), E2005–E2013.
Warren, M. M., & Hartel, R. W. (2018). Effects of emulsifier, overrun and dasher speed on ice cream microstructure and melting properties. *Journal of Food Science, 83*(3), 639–647.
Wu, B., Freire, D. O., & Hartel, R. W. (2019). The effect of overrun, fat destabilization, and ice cream mix viscosity on entire meltdown behavior. *Journal of Food Science, 84*(9), 2562–2571.